Seafloor sediment characterization improves estimates of organic carbon standing stocks: an example from the Eastern Shore Islands, Nova Scotia, Canada~~Seafloor sediment characterization to improve estimate of organic carbon standing stocks in continental shelves.~~

Catherine Brenan[1], Markus Kienast[1], Vittorio Maselli[2], Christopher K. Algar[1], Benjamin Misiuk[~~1,~~3,4], Craig J. Brown[1]

[1]Department of Oceanography, Dalhousie University, Halifax, B3H 4R2, Canada
[2]Department of Chemical and Geological Sciences, University of Modena and Reggio Emilia, Modena, Italy~~Department of Earth and Environmental Science, Dalhousie University, Halifax, B3H 4R2, Canada~~
[3]Department of Geography, Memorial University of Newfoundland, St. John's, A1B 3X9, Canada
[4]Department of Earth Sciences, Memorial University of Newfoundland, St. John's, A1B 3X9, Canada

Corresponding Author: Craig J. Brown (craig.brown@dal.ca)

Abstract. Continental shelf sediments contain some of the largest stocks of organic carbon (OC) on Earth and play a vital role in influencing the global carbon cycle. Quantifying how much OC is stored in shelf sediments and determining its residence time is key to assessing how the ocean carbon cycle will be altered by climate change and possibly human activities~~how human activities can accelerate the process of OC remineralization into carbon dioxide~~. Spatial variations in terrestrial carbon stocks are well studied and mapped at high resolutions, but our knowledge of the distribution of marine OC in different seafloor settings is still very limited, particularly in ~~the highly~~ dynamic and spatially variable shelf environments. ~~The~~ This lack of knowledge reduces our ability to understand and predict how much and for how long oceans sequester CO_2. In this study, we use high-resolution multibeam echosounder (MBES) data from the Eastern Shore Islands offshore Nova Scotia (Canada), combined with OC measurements from discrete samples, to assess the distribution of OC content in seafloor sediments. We derive four ~~three~~ different spatial estimates of organic carbon stock: i) OC density estimates scaled to the entire study region assuming a homogenous seafloor~~,~~ ~~the organic carbon densitystock estimates were scaled to the entire study region~~; ii) interpolat~~ing~~ion ~~the~~ of ~~organic carbon~~ OC density estimates using ~~an~~ Empirical Bayesian Kriging~~ method~~; iii) OC density ~~using a high-resolution substrate map, the estimates were scaled~~estimates scaled to areas ~~to the~~ of ~~areas of~~ soft substrate ~~only~~estimated using a high-resolution classified substrate map~~, ~~; and~~,~~ finally,~~,~~ iv~~ii~~) Empirical Bayesian Regression Kriging ~~using~~ of OC density within areas of estimated soft sediment ~~Empirical Bayesian Regression Kriging prediction~~ to~~, carbon stock estimates~~ ~~OC density in the soft substrate~~only~~ were refined to account for spatial variability in the concentration of OC~~. These four ~~three~~ distinct spatial models yielded dramatically different estimates of ~~average~~ standing stock of OC in our study area of 223 km^2~~, ~~: 80,901~~1275~~, 58,406~~259~~, 16,437 and 6,475~~203~~ ~~M~~t of OC, respectively. Our study demonstrates that high-resolution mapping is critically important for improved estimates of OC stocks on continental shelves, and to the identification of carbon hotspots that need to be considered in seabed management and climate mitigation strategies.

1 Introduction

1.1 Blue~~Marine~~ Carbon

Blue Carbon has received tremendous interest as a natural option for climate change mitigation due to the fact that some marine habitats can store disproportionate amounts of organic carbon (OC) on an area-by-area basis compared to terrestrial habitats (Hilmi ~~*et al*~~*et al*., 2021). The Intergovernmental Panel on Climate Change (IPCC) defines ~~blue carbon~~Blue Carbon as: "*All biologically driven carbon fluxes and storage in marine systems that are amenable to management*." (2019~~Hilmi *et al*., 2021~~). ~~Blue carbon~~By this definition, Blue Carbon is therefore ~~often~~ associated with vegetation in coastal zones, such as tidal marshes, mangroves, and seagrasses (McLeod ~~*et al*~~*et al*., 2011~~Brown *et al*., 2016; Fourqurean *et al*., 2012~~). OC -in m~~M~~arine sediments are often not included in Blue Carbon calculations and definitions since these environments do not sequester carbon via photosynthesis (Lovelock *et al*., 2019 ~~Hunt et al., 2021~~). However, marine sediments are essential carbon reservoirs and regulate climate change by effectively burying ~~organic carbon~~OC over thousands to millions of years if left undisturbed (Berner, 2003~~-~~; Burdige, 2007 ~~Avelar et al., 2017; Fennel et al., 2019; Atwood et al., 2020~~). -Studies are therefore beginning to acknowledge marine sediments as an emerging Blue Carbon ecosystem (Howard *et al*., 2023).

The fate and flux of organic carbon in benthic systems is influenced by a range of factors acting over different timescales (Middelburg, 2018), including natural and anthropogenic-induced processes (Bianchi *et al*., 2021, ~~and~~ 2023). Recent studies have concluded that, on a global scale, ~~fishing activities such as~~ all bottom trawling and dredging ~~can~~ disturbs the seafloor with an estimated 1.47 Pg of aqueous CO_2 emissions (Sala ~~et al~~*et al*., 2021). ~~These~~ However, these estimates have substantial errors (Epstein ~~et al~~*et al*., 2022) and often ignore that the mineralization of benthic carbon stores comes from natural cycles (Hilborn ~~et al~~*et al*., 2023). Combined, t~~T~~hese studies emphasize that further understanding of sediment ocean carbon processes are urgently required to determine if bottom trawling and dredging ~~anthropogenic activities~~ could cause the semi-permanent OC stocks in surficial marine sediments to remineralize back to CO_2 (Bianchi ~~et al~~*et al*., 2023). Also, future ~~further~~ studies into new approaches to determining the distribution of OC are essential to locate areas of carbon-rich seabed. Furthermore, this research could expand the definition of ~~that could become~~ Marine Protected Areas (MPAs) to include areas of high OC stock (Oceans North, 2024).

1.2 Seafloor Substrate

Sediment characteristics, such as mud content, are known to influence the distribution of OC in marine ecosystem (Burdige, 2007; Serrano *et al.,* 2016), with recent studies highlighting ~~that~~the importance of sediment properties ~~are~~ as ~~important~~ predictors of organic carbon storage in Blue Carbon ecosystems (Dahl *et al*., 2016; Krause *et al*., 2022). In shelf environments, where sediment heterogeneity can be high, sediment classification maps may therefore offer a mechanism to determine areas of low and high OC content (Bianchi *et al*., 2021). Multibeam-echosounder (MBES) systems provide information about the environmental characteristics of the seafloor, such as depth, substrate hardness, and sediment characteristics, by collecting bathymetry and backscatter information, which can be used to determine seafloor morphology and as a proxy for seafloor substrate type (Brown ~~et al~~*et al*., 2011). Advancements in MBES have allowed us to create spatially continuous high-resolution maps of the ocean floor (Brown ~~et al~~*et al*., 2011; Buhl-Mortensen ~~et al~~*et al*., 2021; Misiuk and Brown, ~~2023~~2024), at ~~a~~ horizontal resolutions down to sub-meter scales (depending on water depth and sonar specifications; ~~) (~~Mayer ~~et al~~*et al*., 2018). Seafloor sediment mapping ~~is defined as using~~ describes the use of geophysical and physical sampling systems to determine the character of the surface sediments~~,~~ and includes mapping ~~the~~ quantities of clay/silt, sand, gravel, cobble, and boulder using the Wentworth scale ~~-~~ (e.g., ~~Misuik~~Misiuk ~~et al~~*et al*., 2019). ~~The modern~~ Recent methods for producing seabed sediment maps combine high-resolution MBES with ground-truth sampling data using machine learning algorithms (~~Misuik~~Misiuk ~~et al~~*et al*., 2019). Statistical ~~learning~~ techniques include k-Nearest Neighbour (Lucieer ~~et al~~*et al*., 2013; Stephens and Diesing, 2014), Artificial Neural Networks (Huang ~~et al~~*et al*., 2012; Stephens and Diesing, 2014), and Bayesian Decision Rules (Simons and Snellen, 2009; Stephens and Diesing, 2014). The most widely used statistical model for substrate classification and regression maps is Random Forest, due to its ease of implementation and a robust capacity for handling complex, non-linear relationships between environmental variables and ground truthing while avoiding overfitting (Stephens and Diesing, 2015; Misiuk and Brown, ~~2023~~2024).

1.3 Benthic Carbon Mapping

Early marine carbon mapping studies have applied interpolation methods comprising semi-variogram analyses and kriging to spatially predict OC in surficial sediments (Mollenhauer ~~et al~~*et al*., 2004; Acharya and Panigrahi, 2016). More recently, soil ~~organic carbon~~OC has been modeled using multiple methods in terrestrial ecosystems. Mallik ~~et al~~*et al*. (2022) compared artificial neural networks (ANN), Empirical Bayesian Regression Kriging (EBRK), and hybrid approaches combining the two, including ANN-OK (ordinary kriging) and ANN-CK (cokriging). They found that the EBRK method outperformed all other models with highest values of R^2 (0.936) (Mallik ~~et al~~*et al*., 2022). The EBRK method has been widely used in terrestrial soil carbon models but has still not been explored for marine sediment carbon models. More recent studies have utilized ~~MBES and~~ machine learning algorithms to model and map ~~organic carbon~~OC at broad spatial scales at the seafloor (Atwood ~~et al~~*et al*., 2020; Diesing ~~et al~~*et al*., 2017; Smeaton ~~et al~~*et al*., 2019). Diesing ~~et al~~*et al* (2017) used Random Forest to model particulate ~~organic carbon~~OC (POC) at the seafloor using ~~POC~~ measurements from physical seafloor samples, and spatially continuous seafloor environmental variables (500 m grid resolution) covering the Northwest European continental shelf. Similarly, Smeaton ~~et al~~*et al*. (2019) generated a map of seafloor substrate using the F~~f~~olk classification and calculated the OC stock per substrate class (100 m grid resolution). This latter study ~~Smeaton~~ was the only one amongst those listed~~also the only studyone~~ to utilize MBES data to predict OC stock. ~~(Smeaton et al*et al*., 2019).~~ Epstein ~~et al~~*et al*. (2024~~3~~) also ~~used~~ applied Random Forest to model ~~organic~~

~~carbon~~OC stocks and accumulation rates in surficial sediments of the Canadian continental margin at a coarse resolution (200 m grid resolution) and ~~point out~~ emphasize that ignoring the geographic extent of hard substrate (i.e., bedrock) at ~~these~~ such broad spatial scales could inflate carbon stock estimates. These studies have been critical to understanding the carbon hotspots at broad spatial scales, as the traditional lower-resolution maps often lead to oversimplification and inconsistency in carbon averaging. However, understanding distributions of sedimentary OC at a higher spatial resolutions ~~are~~ may be required for effective seabed management strategies (Legge ~~et al~~*et al*., 2020)~~, and~~ .

High-resolution maps ~~(6 m grid resolution)~~ of OC have been produced at a local scale using 48 m resolution backscatter from MBES surveys as a predictor (Hunt ~~et al~~*et al*., 2020~~; Hunt et al~~~~*et al*.~~, 2021). Backscatter can be predictive of seabed sediment properties, and was h~~determined~~ ypothesized to be a proxy for OC based on observed ~~due to extrapolating~~ empirical relationships between ~~sediment~~ grain size and OC, and also potentially other additional sedimentary properties that influence backscatter reflectance (Hunt ~~et al~~*et al*., 2020)~~ and between sedimentary properties and backscatter reflectance~~. Backscatter data may thus be valuable ~~This method could be practical in studies~~ where ~~there are scarce~~ sediment data are scarce. Hunt ~~et al~~*et al*. (2020) indicated that ~~the~~ backscatter ~~data~~ reliably captured information regarding the spatial heterogeneity of the seabed, and that OC correlated strongly with the MBES backscatter signal as a function of sediment composition. However, a more recent study suggested that backscatter distinguishes between coarse and fine sediments (low and high OC) but struggled to differentiate fine-scale variability within finer-grained sediments (Hunt ~~et al~~*et al*., 2021). Differences in results between these studies could be due to the different geographical setting of the studies, limited and asynchronous data, sediment mobility over time, ~~and~~or complex environmental processing of OC in shelf sediments (Hunt *et al*., 2021).

The studies in the North-West European continental margin (Diesing ~~et al~~*et al*., 2017, 2021; Hunt ~~et al~~*et al*., 2020; Hunt ~~et al~~*et al*., 2021; Legge ~~et al~~*et al*., 2020; Smeaton ~~et al~~*et al*., 2021) have shown promising early results. Other studies of carbon stocks have been conducted in the North American ~~Coastal~~ coastal region but without spatially explicit estimates (Fennel ~~et al~~*et al*., 2019; Najjar ~~et al~~*et al*., 2018). Overall, spatially mapping OC at the seabed has only been attempted at a few locations globally, and there is an urgent need to establish robust approaches to ~~conducting~~ obtaining spatial estimates of OC at the seafloor. ~~Furthermore, conducting h~~High resolution OC map~~s~~ping ~~can~~ may additionally help to improve current estimates of seafloor OC stocks and provide insight on marine sediments as an emerging Blue Carbon ecosystem. ~~Our study region, the Eastern Shore islands, is an ideal location since it is an a conservation~~As a conservation Area of Interest (AOI) for the Canadian government, the Eastern Shore Islands (ESI) is an ideal location to test emergent OC mapping methods; it ~~and~~ comprises a heterogenous seabed~~, which~~ that ~~can~~ may provide insight on the effectiveness of various baseline sediment OC estimat~~es of sediment organic carbon~~~~OC~~ ~~in complex seafloor types~~ion and mapping methodologies.

This study addresses three key questions:

1. What is the spatial distribution of seafloor sediment types in the ~~Eastern Shore Islands~~ ESI area?
2. Are seafloor sediments a good high-resolution proxy that enable ~~more~~ accurate estimation of ~~organic carbon~~OC stocks?
3. Does the spatial heterogeneity of substrate type and carbon content influence estimates of ~~carbon~~ OC stock?

2 Study Area

The study region is located within the ~~Eastern Shore Islands (~~ESI~~)~~, ~~an area of interest (AOI) for conservation objectives,~~ approximately 60 km northeast of Halifax (Nova Scotia, Canada, Figure 1). The site stretches from Lower West Jeddore to Fern Hill and extends approximately 25 km from the mainland ~~in the Scotian Shelf region~~ with an area of approximately 223 km^2 (Fisheries and Oceans Canada, 2019) ~~(Jeffery, 2020)~~(Figure 1). The ~~Eastern Shore Islands~~ ESI is a~~n~~ conservation AOI for the Canadian government due to its unique coastal habitat and significant quantities of kelp beds and eelgrass. ~~Also, t~~The estuaries and rivers that drain into the site are considered important habitats for endangered species like Atlantic ~~S~~salmon and juvenile Atlantic c~~C~~od. Furthermore, the hundreds of islands have been identified as an Ecologically and Biologically Significant Area (EBSA), ~~that~~ which providess essential nesting and foraging ground for many colonial seabirds and shorebirds, including ~~h~~ purple sandpiper, and ~~R~~roseate tern, which are endangered according to the Species at Risk Act (Fisheries and Oceans Canada, 2019).

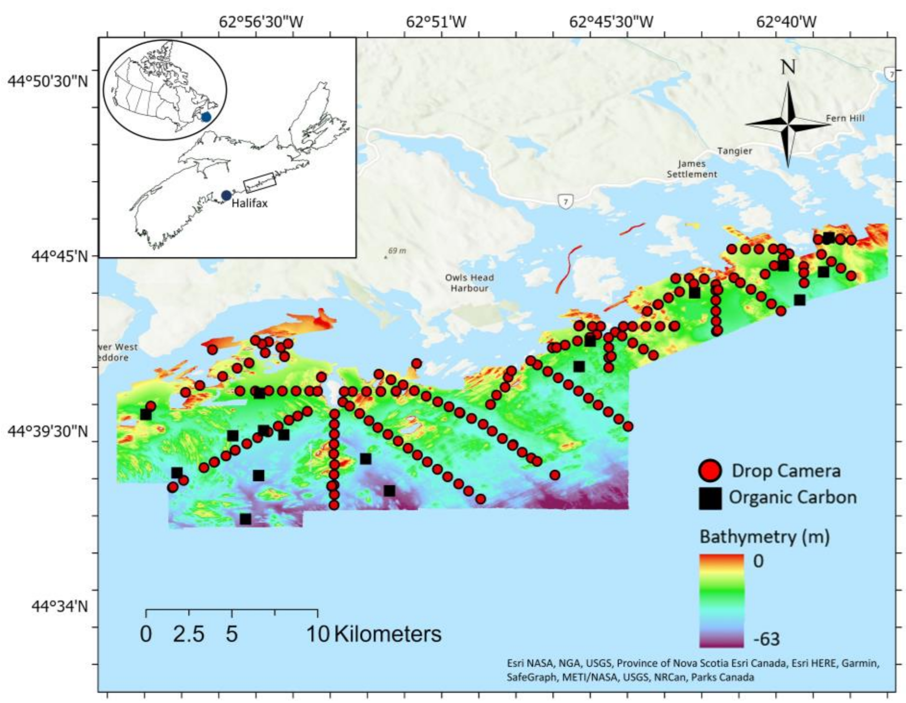

Figure 1. Seafloor MBES bathymetry and sample locations ~~outlining the geographical extent~~ for the survey area ~~within~~ at the Eastern Shore Islands, ~~on the east coast of~~ Nova Scotia, Canada (inset). ~~The drop camera~~

~~imagery is signified by red points and the blue points are the organic carbon~~OC ~~samples. The inset map shows the location in the context of Nova Scotia. (Basemap: Esri NASA, NGA, USGS, Province of Nova Scotia Esri Canada, Esri HERE, Garmin, SafeGraph, METI/NASA, USGS, NRCan, Parks Canada)~~

The study area has a water depth between 31 and 63 m. ~~The seafloor is characterized by bedrock, at places covered by a layer of sediments of varying grain size (from clay to boulders) and thickness (King, 2018).~~ The surficial geology of the ~~-~~ESI ~~surficial geology has~~ is ~~high~~ spatially ~~variability and is~~ heterogeneous, with bedrock overlaid by mud, sand, gravel, cobble, and boulder substrates~~.~~ ~~The seabed character of the ESI is primarily bedrock since it continues from the geomorphology of the land~~ (King, 2018). The bedrock topography is an extension of the terrestrial geomorphology and heavily influences the type and distribution of the surficial deposits. The glacial imprint is substantial in the area, ~~depositing~~having deposited a sequence of till and glaciomarine mud, which lie directly on the bedrock (King, 2018). There is also a thin layer of wave-modified sand and gravel, and more recent deposits of estuarine mud derived from coastal erosion (Fisheries and Oceans Canada, 2019). ~~The ESI surficial geology has high spatial variability and is heterogeneous, with bedrock overlaid by mud, sand, gravel, cobble, and boulder substrates.~~ Ocean surface temperatures in the ESI are around 1° C in winter for the 0–100 m depth range and increase in the summer with some stratification leading to surface temperatures exceeding 15° C (Fisheries and Oceans Canada, 2019) ~~(Jeffery, 2020)~~. By the fall, mixing deepens this warm layer. Ocean currents run predominantly southwestwards ~~on the ESI~~, with some fluctuation around the coast (Feng ~~et al~~*et al*., 2022). The combination of upwelling, currents, and wind allows for the mixing of nutrients, acting as an essential component of the marine food web in the region (Fisheries and Oceans Canada, 2019) ~~(Jeffery, 2020)~~. Nutrients are derived from river, coastal runoff and mixing. They are depleted in the spring due to phytoplankton blooms and replenished in the fall when upwelling is predominant (Fisheries and Oceans Canada, 2019) ~~(Jeffery, 2020)~~. Major human~~anthropocentric~~ activities in this area include lobster fishing, recreational fishing, and boating, but the human impact is low due to low population density and reduced coastal development compared to nearby Halifax and St. Margaret's Bay (Fisheries and Oceans Canada, 2019). ~~(Jeffery, 2020).~~

3 Materials and Methods

To quantify OC stock in the ESI, sediment samples were collected, and OC content and sediment grain size were measured. OC density was calculated for each sample, and four OC stock estimations were generated. The first assumed a homogenous seafloor by scaling up the average OC density to the entire study area. The second also assumed a homogeneous seafloor~~,~~ but used Empirical Bayesian Kriging (EBK) to derive the spatial variability of OC density for the study area. Both scenario 1 and 2 were conducted to evaluate OC estimates when no high-resolution mapping data is available. To further refine the OC stock estimates, a substrate classification map was developed by combining high-resolution seafloor predictor variables (derived from multibeam sonar data – see below) and subsea camera imagery of the seabed. The substrate classification map partitioned the study area into hard and soft substrates. The third OC stock estimate utilized the sediment classification and scaled the average

OC density to the area of the soft substrate. The final OC stock estimate also utilized the sediment classification map but used ~~and an EBRK regression~~ Empirical Bayesian Regression Kriging (EBRK) prediction to ~~assess~~ incorporate the spatial variability of the OC density within the soft substrate only. Scenarios 3 and 4 determine OC estimates when sediment information and high-resolution mapping data is available. ~~The general~~ An overview of the ~~data processing~~ analysis workflow is shown in Figure 2.

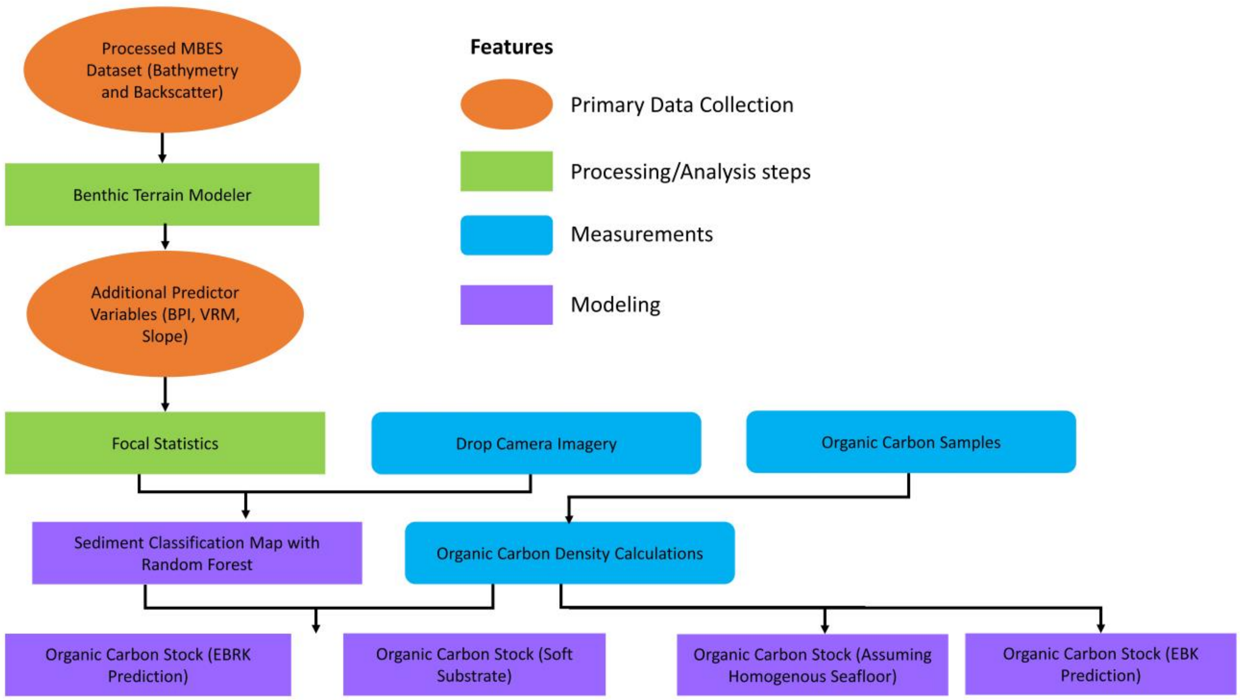

Figure 2. ~~Flow chart outlining the geoprocessing~~ General analysis steps used to estimate organic carbon ~~determine the carbon estimates for all~~ for four scenarios. ~~Chart shows data inputs and outputs, processing steps, measurements, and modelling.~~

3.1 Hydrographic Datasets

MBES data were collected by the Canadian Hydrographic Service over two separate surveys (20 June – 29 July 2019; 17 August – 05 September 2020) (Bondt, 2019, ~~; Bondt,~~ 2020). Three launches were used to complete this survey – the *CSL Kestrel, CSL Tern* and *CSL Pelican*. The survey launch *CSL Kestrel* was equipped with an R2Sonic 2022 multibeam echosounder. The survey launches *CLS Tern* and *CSL Pelican* were outfitted with Kongsberg EM2040C and EM2040C Dual Head echo sounders, respectively. All surveys were conducted at MBES operating frequencies of 200-400kHz. Vessel position and orientation were corrected in real time by Trimble/Applanix POSMV V5 motion compensation systems. Echosounder data was corrected for sound velocity in real time using Applied Microsystems Limited sound velocity sensors. The vessel position was recorded in real-time using the CANNET RTK NTRIP connected directly through the POSMV. Raw position and orientation data from the POSMV were logged throughout the survey for further post-processing where required. Bathymetry and backscatter data were processed using the QPS software suite. Bathymetry data were processed in ~~QIMERA~~ Qimera 2.5.3 to generate a bathymetric digital elevation model (DEM) for the survey area. Backscatter data were processed in FMGT 7.10.2 to generate backscatter mosaics for each of the data sets. Backscatter data were not calibrated; the different survey data sets were harmonised using bulk shift methods (Misiuk ~~et al~~*et al*., 2020, 2021; Haar ~~et al~~*et al*, 2023) from areas of overlap between the survey data sets to generate a corrected backscatter mosaic for the entire study area.

Seafloor morphology features were derived from the primary bathymetric datasets to provide additional predictor variables for ~~the~~ sediment classification modelling. These were selected based on literature review, expert suggestions, and access to data, and were calculated using ArcGIS Pro 3.1.2 ~~and~~ using the Benthic Terrain Modeler (BTM) 3.0 Toolbox. The terrain features included slope, bathymetric position index (BPI) and vector ruggedness measure (VRM), which are considered ~~successful~~ useful predictors ~~in previous~~ for seabed substrate classification ~~studies~~ (Stephens and Diesing, 2015; Misiuk ~~et al~~*et al*, 2019) (Table 1) (Figure 3~~2~~). The Focal Statistics tool was used to obtain the mean value for each ~~for all the~~ predictor variables over ~~and calculated for each input cell location~~ a~~using statistics of the values within a specified neighbourhood (ArcGIS Pro, 2023). In this study, a rectangle neighbourhood type of~~ a 20 by 20 pixels neighbourhood ~~calculated the mean pixel value, which helped smooth the surface and~~ to reduce noise~~ in the predictor variables~~. ~~These~~ The ~~predictor~~ variables were then used in both the substrate map and the ~~organic carbon~~OC model. ~~The environmental variables were determined based on literature review, expert suggestions, and access to data.~~

Table 1. Description of predictor variables used to model sediment type~~, including their units and description~~.

Environmental Variables	Description	Resolution	Units
Bathymetry	Depth of the seafloor	2 m	meters
Backscatter	Measure of intensity of acoustic signal from MBES and indicator of bottom hardness	2 m	relative dB
Slope	Measures maximum change in elevation (steepness)	2 m	degrees
Vector Ruggedness Measure (VRM)	Measures terrain ruggedness of grid cells within a neighbourhood	2 m	meters
~~Broad~~ Bathymetric Position Index (BPI)	Differences in values of centre cell to mean of surrounding cells.	2 m	meters

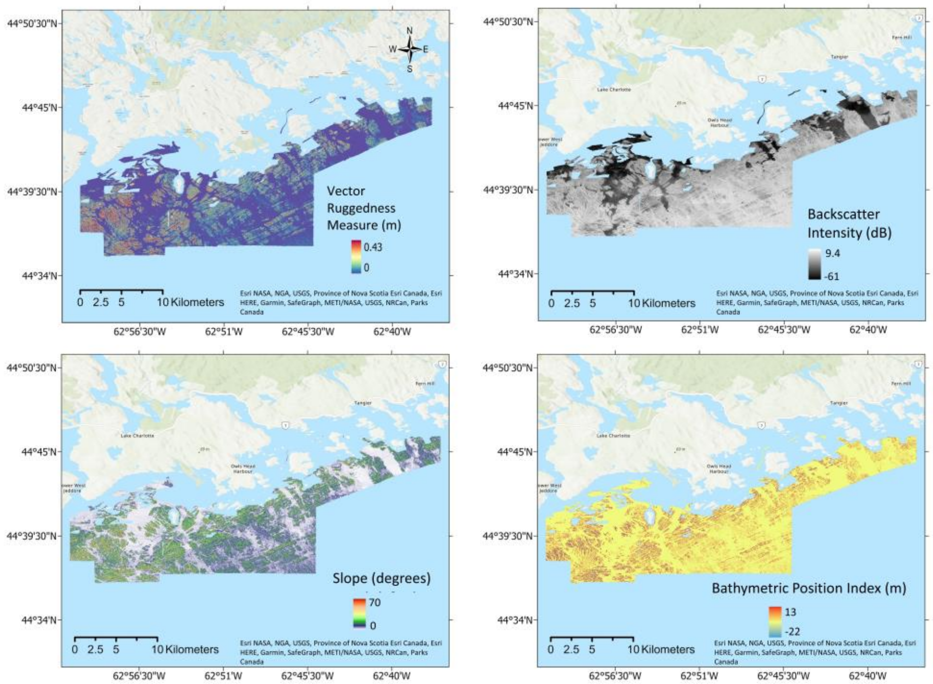

Figure 3~~2~~. Backscatter, Slope, VRM and BPI data mapped in the Eastern Shore Islands study area.~~ (Basemaps: Esri NASA, NGA, USGS, Province of Nova Scotia Esri Canada, Esri HERE, Garmin, SafeGraph, METI/NASA, USGS, NRCan, Parks Canada)~~

3.2 Seabed S~~s~~ediment S~~s~~ampling

Sampling surveys for OC and grain size were conducted between 9 - 27 May 2022 from the *MV Island Venture*. ~~A stratified random sampling technique was used~~Sampling locations were randomly placed in regions of low MBES backscatter~~ based on the backscatter mosaic~~, which indicate softer, unconsolidated sediments where grab sampling ~~by grab sampler would ~~should be ~~achievable ~~successful ~~ ~~(Figure 3~~2~~). Acoustic backscatter was used to select sampling locations ~~since it is a~~~~can be ~~as a ~~good ~~proxy ~~of ~~for sediment grain size ~~and is commonly used in substrate classification routines ~~(Goff *et al*., 2000; Sutherland *et al*., 2007; Collier *et al*., 2014; Hunt ~~et al~~*et al*., 2020). A 0.1 m^2 Van Veen grab ~~sampler sampling to a maximum depth of 20cm was ~~fitted with a GoPro camera was operated to collect sediment samples and drop camera imagery at each sample location, with the grab penetrating up to ~10 cm depth into the substrate. The GPS position of the research vessel was recorded at the point of contact ~~on ~~at the seabed at each grab station. A total of 17 g~~G~~rabs ~~deployments ~~were ~~done only ~~successful in areas of soft substrate~~ where it was possible to retrieve a sample ~~. Generally, it is difficult to sample a coarser sediment matrix successfully, and these sediment types are often under-represented in sedimentary carbon studies (Hunt ~~et al~~*et al*., 2020). After thoroughly mixing the sediment in the Van Veen grab, 0.907 kg subsamples of sediment were taken from the grabs, and each placed in a ~~32 oz~~ plastic container for ~~organic carbon~~OC analysis. Following collection, these samples were stored in a cooler during the day and put into a freezer in the evening.

3.3 Processing of S~~s~~ediment G~~g~~rab S~~s~~amples

Prior to sediment grain size and OC analysis, the samples were dried from frozen in the oven at 60~~-~~° C overnight and kept in a dark dry cabinet. ~~The s~~Sedimentary OC from the grab samples was quantified using an elemental analyzer (EA, Elementar Microcube~~-microcube~~) with a detection limit of 0.03 mg. Based on the method ~~from~~ of Verardo ~~et al~~*et al*. (1990), a section of the grab samples (~~five~~ 5 ~~grams~~g) ~~were dried in the oven at 60° C overnight and~~ ~~were~~ was ground using a mortar and pestle to form a homogenous powder. ~~Coarse-grained sediments (above >2 mm diameter) were excluded since they are too large for elemental analysis.~~ Two samples (ES-31, ES-35) ~~had~~ contained significant concentrations of sediment grains coarser than 2 mm ~~notable amounts of course-grained sediments~~ (around 30% of sample).~~>~~ These sand grains were removed using mesh sieves prior to grinding and EA analysis, but final sedimentary OC concentrations were adjusted to total sample weight following EA analysis. ~~The coarse fraction was removed from these samples using a mesh sieve and the % OC adjusted accordingly.~~ Silver capsules were used to weigh the initial mass (0.5-0.7 mg), and acid fumigation was performed by exposing the samples to 37% hydrochloric acid (HCl) to remove any inorganic carbon ~~(IC)~~. ~~It is significant to note that an acid wash could also potentially remove some OC content, which could alter the results (Verardo et al., 1990).~~ These capsules were then placed in an oven overnight at 60° C before ~~undergoing~~ analysis.

The remaining section of the grab samples was used for s~~S~~ediment grain size analysis, ~~and was conducted using~~following the protocol ~~derived from~~~~by~~of Mason (2011). The sediment was first split into pebble/cobble (>4000 µm), gravel (>2000 µm) and fine sediment (<2000 µm) material using mesh sieves. The fraction <2000 µm was evaluated using a Beckman Coulter~~’s~~ LS 13 320 particle size analyzer at the Bedford Institute of Oceanography. Following the guidance ~~by~~ of Mason (2011), the samples were not treated with acid or hydrogen peroxide because the samples had relatively low organic content~~based on the OC analysis, of the samples had relatively low organic content~~. The results from the coarse and fine-scale fractions were combined into a full particle size distribution to determine the percentage~~s~~ of mass of the total for each sample~~the different sediment types~~ (supplementary material). It should be noted that dry bulk density was ~~unable to be~~ not measured directly in this study ~~and~~but was instead calculated (see section 3.6).

3.4 Subsea V~~v~~ideo S~~s~~urveys

A total of 174 drop camera ~~stations~~ videos were ~~conducted~~ collected by Fisheries and Oceans Canada (DFO) over 13 days during September and October 2017 aboard the vessel *RV Sigma-T* (Fisheries and Oceans Canada, 2019). ~~(Jeffery et al., 2020)~~ (Figure 1). A~~n~~ HD subsea video camera (SV-HD SDI) was used with ~~which recorded~~ camera time and position~~al information using~~ recorded using a video overlay streamed from the chart plotter~~(Proteus II), where it received positional and time/date stamp data from the chart plotter~~ (Vandermeulen, 2018). ~~The overlay sent t~~The ~~completed~~ video feed with overlay outputted to a direct-to-disk HD recorder and a standard low-power LED TV. The GPS antenna for the navigation system was mounted on the roof of the wheelhouse approximately 10 m ~~distant~~ from the drop camera when deployed off the stern gallows. In this manner, all positional information in the video overlay ~~would be~~ was offset by ~~at least~~ ~10 m and ~~. This offset~~ was adjusted ~~when reviewing the~~

~~data~~during post-processing ~~accounted for in subsequent analyses~~. ~~Drop camera targets from the GIS were labelled and embedded into the *RV Sigma T* navigation computer.~~ Approximately three minutes of moving video was recorded at each drop camera location ~~with the camera light turned on~~. ~~Due to the camera moving, the location would change in small increments, therefore the location in the~~ The centre ~~middle~~ of each video drift was recorded as the station location. All the drop camera sites ~~were~~ occurred at depths ~~greater than~~ > 10 m. ~~Additionally, t~~The GoPro camera imagery ~~of the seafloor~~ collected ~~from the GoPro camera fitted to~~ with the grab sampler during ~~the sampling of organic carbon~~OC sampling in 2022 (see sediment sampling section above) was ~~also~~ additionally incorporated with the drop camera imagery ~~conducted by DFO~~ for subsequent analysis (Figure 1).

From each video station, a presence (1) and absence (0) of different sediment types were recorded in post processing. The data was classified into two sediment types: h~~H~~ard substrate (rock, boulder, cobbles, pebbles, and gravel), and soft substrate (mud and sand) (Figure 4~~3~~) (supplementary material).

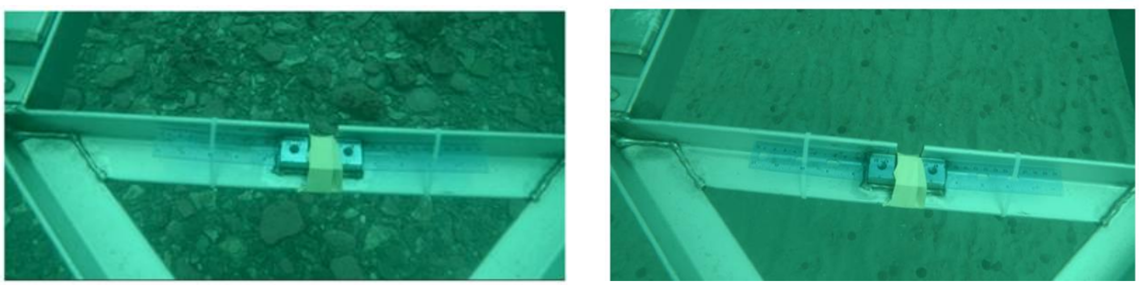

Figure 4~~3~~. Example of seafloor imagery from each of the two substrate classes: h~~H~~ard Substrate (left); soft substrate (right). Photos from a GoPro camera mounted on the ~~van~~ Van ~~veen~~ Veen grab. Width of images are approximately 0.5 m, with the frame of the grab providing scale for classification of substrata.

3.5 ~~Sediment Modelling~~ Sediment Classification Model

Random Forest has been used in previous carbon mapping studies due to its high predictive accuracy, capacity to manage many predictor variables, and unbiased internal validation (Diesing ~~et al~~*et al*., 2017). In our study, Random Forest was used to model the sediment grain size ~~type~~class to inform ~~, which would then provide insight into areas with high~~ OC content estimation~~. Random Forest was performed~~ ~~here~~ using R version 4.3.1 with the randomForest package (Liaw and Wiener, 2002). The model was initially trained with default hyperparameters ($ntree = 500$, $mtry = 2$, $nodesize = 1$) using the substrate classification observations and all predictor variables (bathymetry, backscatter, BPI, VRM and slope). Random Forest is an ensemble modelling approach comprising many individual classification trees, each grown on a bootstrapped version of the dataset. The observations not selected for a given tree are termed the "out-of-bag" (OOB) observations. Given enough trees, each response observation will be represented in the OOB sample multiple times. By predicting the OOB values for each individual tree during model training, the results can be aggregated over all trees to provide a useful set of validation predictions that were not used to inform training~~have not been exposed to training observations~~. The OOB observations were used here to estimate predictor variable importance by permuting the predictor values and measuring the resulting increase in OOB error (Liaw and Wiener, 2002). Random Forest is generally considered robust to the use of correlated predictors and estimates of importance additionally suggested contribution to the model by all variables, which were thus retained. Informal trials suggested that a model of 100 trees (i.e., $ntree = 100$) provided sufficient predictive capacity but improved computational speed. After training the final model with these parameters, a confusion matrix was generated using the OOB observations and predictions to evaluate the map accuracy, and the model was then predicted across the full map extent using the predictor variable rasters. The ~~performance~~ kappa statistic was used to evaluate the ~~Random Forest~~ model ~~was Kappa~~predictions, ~~which indicates~~ indicating how ~~much~~ well ~~observers~~ predictions agree with observations beyond the level of agreement that could be expected by chance: ~~and is calculated from:~~

$$k = \frac{\rho_o - \rho_e}{1 - \rho_e} \qquad (1)$$

where κ is the value of kappa between −1 and 1, po is the proportion correctly classified and pe is the proportion correctly classified due to chance, based on the frequency of observations and predictions of each class ~~(Misiuk, 2019)~~. A k~~K~~appa ~~=~~score of ~~0.0~~0 ~~should be taken as representing~~ is considered “poor” agreement, ~~between~~ while values in the range ~~0.000~~ ~~and~~ to 0.20 ~~as~~ are often considered “slight” agreement, 0.21 ~~±~~to 0.40 as “fair” ~~agreement~~, 0.41 ~~±~~to 0.60 as “moderate” ~~agreement~~, 0.61 ~~±~~to 0.80 as “substantial” agreement, and 0.81 ~~±~~to 0.99 as “almost perfect” agreement. ~~A kappa coefficient of 1 represents perfect agreement (McHugh, 2012).~~

3.6 Estimation of ~~Total Standing Stock of Organic Carbon~~ Standing Stock of Organic Carbon

The elemental analyser reports OC value as a proportion (weight %). ~~Previous studies have stated that an arcsine transformation on the OC value (X) is advisable since it can make the variance constant and the data appears normally distributed (Sokal and Rohlf, 1981; Diesing et al~~*et al*~~., 2017):~~

~~$Y = \arcsin\sqrt{X}$ (1)~~

Dry bulk density was not measured directly in this study but calculated from estimated porosity and density. Porosity (Φ) ~~is~~ was calculated from predicted mud content (dimensionless fraction), which is a combination of clay and silt from the grain size distribution measurements using the equation (2) derived from Jenkins (2005).

$$\Phi = 0.3805 * C_{mud} + 0.42071, \qquad (2)$$

where Φ and C_{mud} (mud content) are dimensionless fractions. The equation was derived based on data from the Mississippi-Alabama-Florida shelf, and it is assumed that the equation is not site-specific (~~e.g.,~~ Diesing ~~et al~~*et al*., 2017).

Dry bulk density (p_d) of the sediment was estimated using the porosity and sand grain density (p_s= 2650 kg m^{-3}) (Diesing ~~et al~~*et al*., 2017; Hunt ~~et al~~*et al*., 2020):

$$p_d = (1 - \Phi)\, p_s \qquad (3)$$

The organic carbon density (kg m^{-3}) was calculated by multiplying the %OC (Y) (expressed as a decimal proportion) by the sediment dry bulk density (p_d). Following prior studies that quantified marine sedimentary ~~organic carbon~~OC (e.g., Diesing 2017, Hunt 2021), the ~~standing stock of organic carbon~~ standing stock of organic carbon ~~(m_{OC})~~ per grid cell (m_{OC}) was estimated by multiplying the average OC density by ~~the transformed organic carbon% OC (expressed as a decimal proportion) concentration (Y), dry bulk density (p_d),~~ the ~~average~~ sampling depth of the Van Veen grab ($d = 0.1$ m), ~~and~~ area of mapped grid cell ($A = 4$ m^2) and converted to metric tonnes (divided by 1000) using the equation (4) below:

$$m_{OC} = (Y * p_d * d * A)/1000 \qquad (4)$$

Finally, the total standing stock was the m_{OC} multiplied by the total pixels in the study site (scenarios 1 and 2) or the total pixels in the soft substrate (scenarios 3 and 4).

3.7 Spatial Interpolation of Organic Carbon ~~(no substrate map~~ – No Substrate~~)~~

After the m_{OC} was calculated for each sample, EBK was used to spatially interpolate m_{OC} within the entire study site. EBK is a geostatistical interpolation method that builds a ~~valid~~ kriging model by subsetting the study area, coupled with multiple simulations to obtain the best fit (Krivoruchko and Gribov, 2019). This process finally creates several simulated semi-variograms, ~~and each semi-variogram~~ each of which is an estimate of the true semi-variogram for the subset (Pellicone *et al*., 2018). EBK differs from other kriging methods since it considers the uncertainty in the semi-variogram estimation step, ~~which provides~~ providing an ~~accurate~~ estimate of the prediction standard errors ~~of prediction~~. An exponential semi-variogram and an empirical transformation were selected ~~The data were transformed empirically~~ and EBK was executed in the geostatistical wizard in ESRI ArcGIS Pro 3.1. ~~Also, an empirical transformation was applied to lower the error and cross-validation results.~~

3.8~~7~~ Spatial Interpolation of Organic Carbon Density – Soft Substrate ~~in the soft substrate~~

EBRK was used for the spatial interpolation of **OC density** ~~m_{OC}~~ and estimation of values at unknown locations within the extent of the soft substrate. EBRK is a geostatistical interpolation method that combines ordinary least square regression and kriging to provide accurate predictions of non-stationary data at a local scale (Giustini ~~et al~~*et al*., 2019). An exponential semi-variogram model and an empirical transformation were selected for the EBRK model ~~was performed since it provided the lowest error in the cross-validation results.~~, which was ~~EBRK was performed in the geostatistical wizard in ESRI ArcGIS Pro 3.1. The EBRK model was~~ evaluated using leave-one-out cross-validation (Mallik ~~et al~~*et al*., 2022). The EBRK method is different from EBK ~~since you can add~~ in that predictor variable information is ~~s into~~ accommodated by including their principal components as regression variables prior to the kriging step~~the model~~. Thus, all the predictor variables from the substrate classification map (bathymetry, backscatter, bpi, vrm and slope) were masked to the soft substrate area ~~using the extract by mask tool~~ in ESRI ArcGIS Pro 3.1 and ~~added~~ included in the EBRK ~~to the~~ model to improve estimation of OC density estimations. ~~The model was validated according to the mean error (ME) and the root-mean-square error (RMSE). ME is the average of the cross-validation errors, measures model bias and should have a value close to zero (Acharya and Panigrahi, 2016). RMSE is defined as the square root of the average squared prediction errors and measures prediction accuracy. .~~

3.9 Cross Validation Methods

To ~~evaluate~~estimate the ~~prediction~~ accuracy of the ~~cross-validation method for the~~ EBK and EBRK predictions, the mean error (ME) and the root-mean-square error (RMSE) were calculated. ME is the average of the cross-validation errors, measures model bias and should have a value close to zero (Acharya and Panigrahi, 2016).

$$ME = \frac{1}{n}\sum_{i=1}^{n}\{z(xi) - \hat{z}(xi)\} \qquad (5)$$

RMSE measures the difference between the predicted and the observed values and estimates the standard deviation of the residuals (Boumpoulis *et al*., 2023). A small root mean square error (RMSE) indicates that the model has performed well and can predict the data accurately.

$$RMSE = [\frac{1}{n}\sum_{i=1}^{n}\{z(xi) - \hat{z}(xi)\}^2]^{1/2} \qquad (6)$$

The z(xi) is the observed OC and $\hat{z}$ (xi) is the prediction of OC at location xi, and n is the number of observations. ~~Statistical parameters of the~~ These cross-validation error parameterss were calculated ~~using~~ within the Geostatistical Wizard Tool in the ESRI ArcGIS Pro 3.1 ~~software~~.

4 Results

4.1 Grain size Distributions, Sediment Properties, and Organic Carbon Content~~Concentrations~~

Van Veen grab samples provided grain size and ~~organic carbon~~OC measurements at each station (Table 2). It is important to note that silt and clay were merged into a single mud class to estimate the OC stock (Burdige, 2007; Hedges ~~&~~and Keil, 1995).

Table 2. Raw data from grab samples including grain size and ~~organic carbon~~OC measurements.

Station	>4000 um (%)	>2000 um (%)	Sand Content (%)	Silt Content (%)	Clay Content (%)	Porosity	Dry Bulk Density (kg/m^3)	Organic Carbon Content (%)
ES-02	0.27	0.08	54.3	38.4	7.13	0.59	1077.6	1.22

ES-03	0.003	0.06	90.8	7.11	2.03	0.46	1443.0	0.12
ES-04	0.33	0.01	93.7	4.28	1.69	0.44	1475.1	0.13
ES-07	0.00	0.00	24.4	65.2	10.3	0.71	773.0	1.85
ES-15	0.59	0.11	94.6	3.44	1.29	0.44	1487.4	0.06
ES-17	2.07	0.30	63.7	30.5	4.18	0.55	1185.1	0.10
ES-18	0.60	0.04	80.2	17.4	1.93	0.49	1340.5	0.23
ES-19	0.00	0.04	96.7	2.15	1.12	0.43	1502.2	0.08
ES-21	0.14	0.10	91.4	7.23	1.17	0.45	1450.4	0.06
ES-23	0.08	0.21	93.8	4.68	1.27	0.44	1475.1	0.07
ES-25	0.006	0.01	95.4	3.50	1.05	0.44	1489.3	0.05
ES-27	0.04	0.05	85.0	13.3	1.67	0.48	1384.7	0.07
ES-28	0.00	0.05	85.2	13.2	1.63	0.48	1385.8	0.08
ES-29	0.00	0.02	86.7	11.4	1.87	0.48	1401.4	0.08
ES-31	21.42	9.97	45.8	22.2	1.11~~4.78~~	0.51	1199.2	0.57
ES-34	2.15	0.71	52.4	39.9	6.15	0.59	1071.1	0.61
ES-35	34.00	0.37	17.3	44.0	4.26~~8.83~~	0.61	793.01	0.62

4.2 Relationship between Grain S~~s~~ize and Organic Carbon ~~-~~Content

A linear regression~~n~~ ~~ordinal least square regression (OLS)~~ was performed to examine the relationship between OC content (%) and the percentage grain size composition of mud. There was a significant positive relationship between OC content and percent mud ($p<0.001$; $R^2=0.81$) (Figure 5~~4~~), suggesting that, ~~here,~~ % mud content ~~sediment type~~ may be useful as a proxy for OC content, as also observed at many other sites (Burdige, 2007; Hedges ~~&~~ and Keil, 1995; C. A. Hunt ~~et al~~*et al*., 2021).

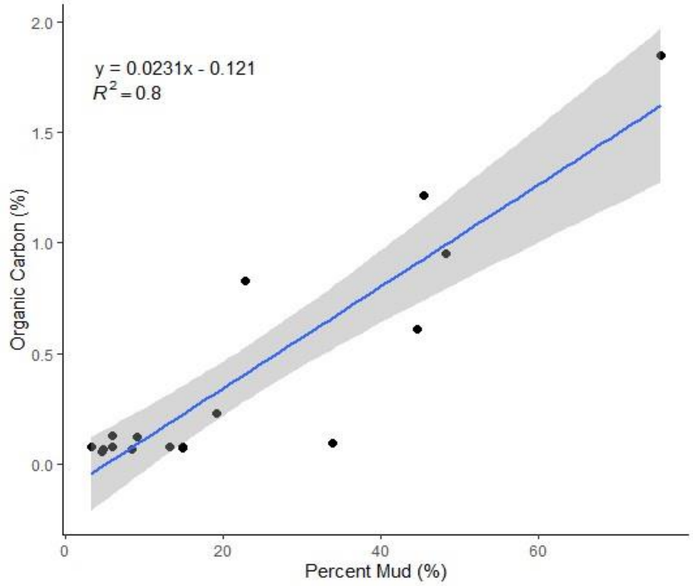

Figure 5~~4~~. Linear regression indicating the relationship between OC and percent mud ~~(top right)~~. The grey area represents a 95 percent confidence interval for the slope of the regression line.

4.3 Substrate Classification Map

Outputs from Random Forest indicated that bathymetry, backscatter, vector ruggedness measure (VRM) and slope were all important for the sediment classification. Figure 6~~5~~ shows the relative ~~significance~~ importance of the five variables ~~t~~in the model~~o prediction accuracy~~. Backscatter was the most important variable for predicting sediment type, followed by VRM, slope, bathymetry, and BPI.

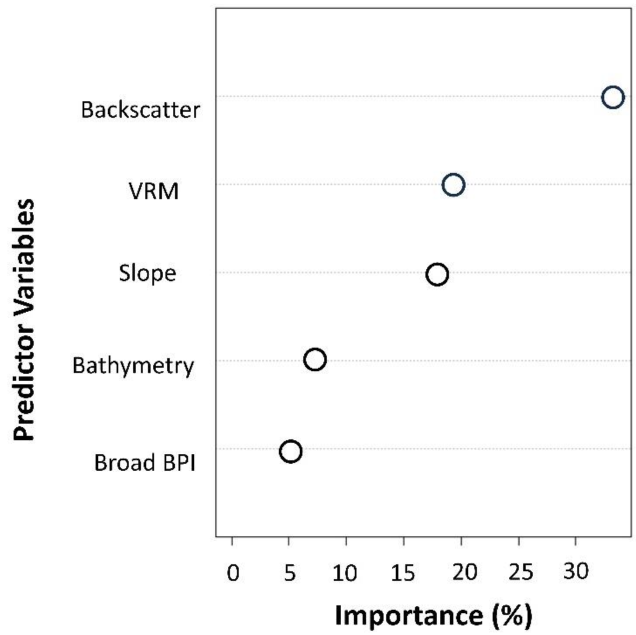

Figure 6~~5~~. ~~Variable iImportance scores.~~ The importance of predictor variables as ~~indicated by the~~ estimated using Random Forest~~ algorithm~~. ~~The y axis indicates the variables of the final model, the x-axis indicates the relative percent importance.~~

The confusion matrix calculated using the OOB observations is presented in Table 3. ~~The~~ A k~~K~~appa score ~~was~~ of 0.69 ~~and F1 was 0.91 (Table 4). This~~is ~~ese statistics indicates~~ indicates that ~~there was~~ substantial agreement between observations and predictions of each class, ~~the OOB samples were predicted with high accuracy (87%) and precision (89%),~~ suggesting that the model was able to successfully differentiate soft and hard substrates within the study area.

Table 3. Confusion ~~Matrix~~ matrix of ~~sediment map~~ substrate type predictions~~to assess the level of agreement between the observed drop camera imagery values and the mapped sediment type~~.

		Observed ~~Drop Camera Imagery~~ ~~Actual Values~~	
		Hard Substrate	Soft Substrate
~~Predicted Values~~ Mapped Predicted ~~Sediment Type~~	Hard Substrate	129	16
	Soft Substrate	9	44

~~**Table 4. Performance of Substrate Model**~~

~~Substrate Classification~~	~~Kappa~~
	~~0.6909~~

The sediment classification map revealed that the hard substrate was the most spatially extensive (178 km^2) whereas the soft substrate class was smaller, covering approximately 45 km^2 of the study area, corresponding with contiguous patches of relatively low relief seafloor (Figure 8). Sediment grain size from the grab samples revealed grain size ~~average~~ percentiles d_{10}=17 um, d_{50} = 147 um and d_{90} = 1822 um. This suggests predominantly sandy ~~that most~~ sediments~~ samples were represented by sand~~, with varying smaller proportions of silt and clay (Figure 7). Two samples were comprised of around 30% coarse substrate~~gravel~~ (>2000 um) (Figure 7).

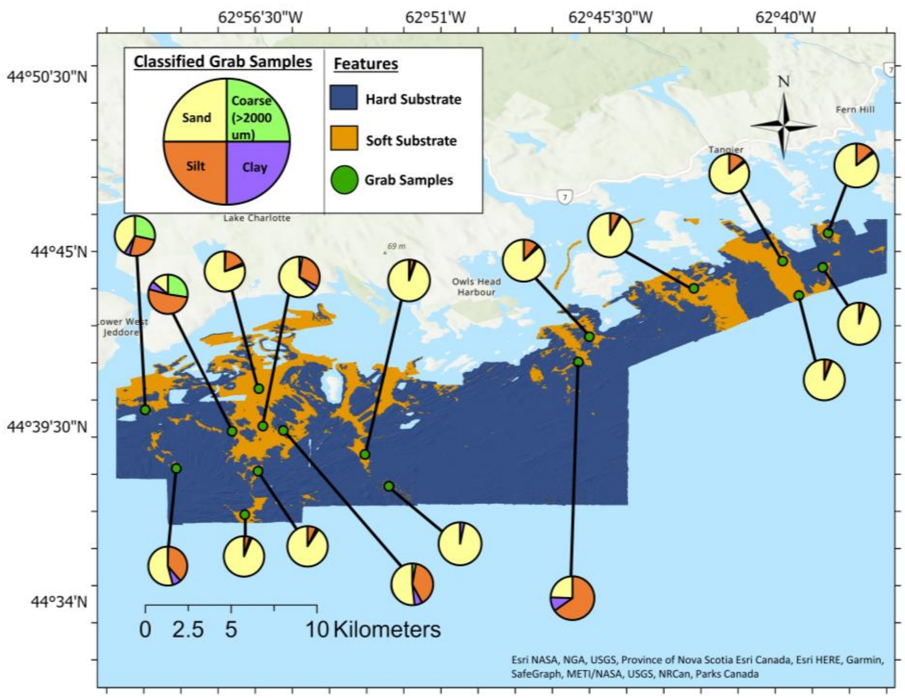

Figure 7. Sediment classification map indicating predicted soft ~~hard~~ (orange) and hard~~soft~~ (blue) substrates~~substrate (bluepurple)~~. Pie charts depict ratios of sand (yellow), silt (orange red), clay (purple),~~ pebble/cobble (blue),~~ and coarse ~~gravel~~ (green) ~~found in~~ for each sediment sample collected.~~ (Basemap: Esri NASA, NGA, USGS, Province of Nova Scotia Esri Canada, Esri HERE, Garmin, SafeGraph, METI/NASA, USGS, NRCan, Parks Canada)~~

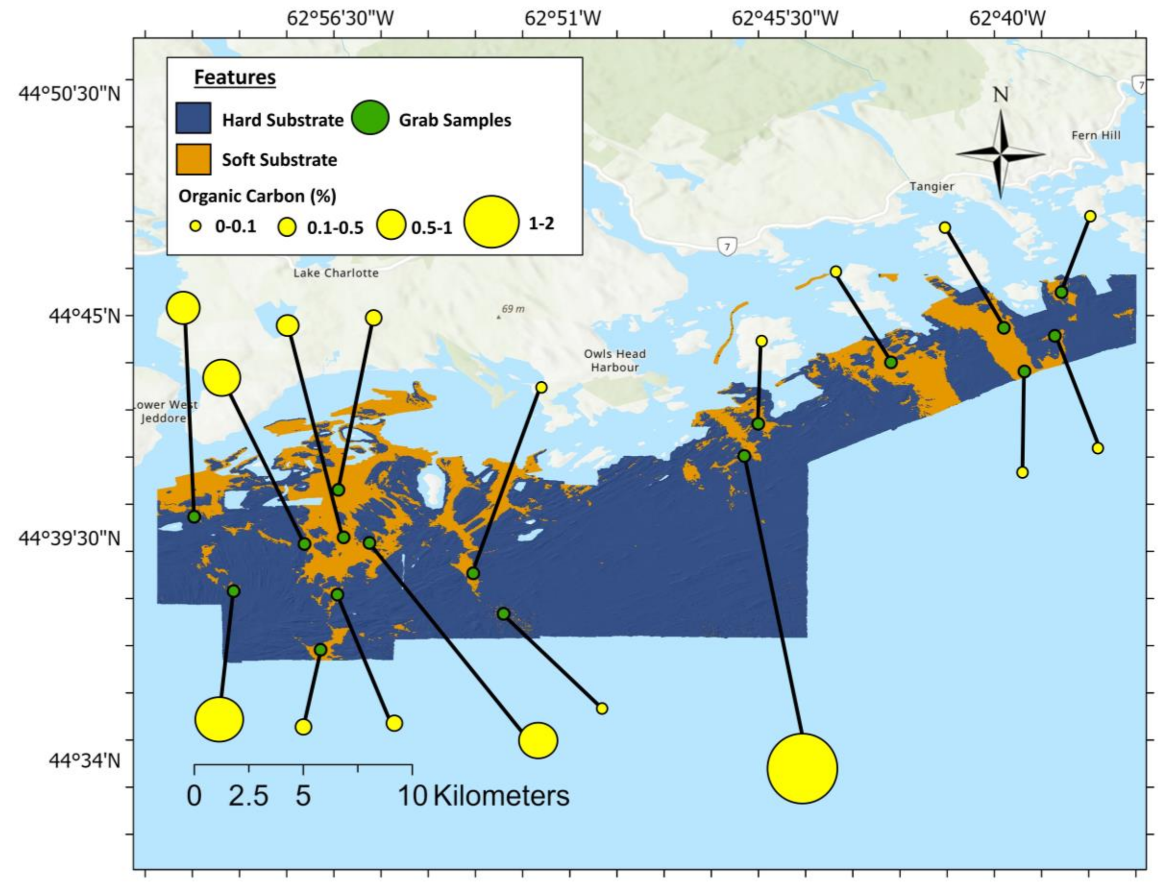

Figure 8. Sediment classification map indicating areas of soft (orange) and hard (blue) substrate ~~(blue)~~. Proportional symbols of OC indicate the sampled percentage (yellow). ~~(Basemap: Esri NASA, NGA, USGS, Province of Nova Scotia Esri Canada, Esri HERE, Garmin, SafeGraph, METI/NASA, USGS, NRCan, Parks Canada)~~

4.4 Organic Carbon Density ~~Prediction~~ Maps

Predicted OC density was high on the west part of the study site near lower west Jeddore and in the middle of the study area near Owls Head Harbour (Figure 9). Cross-validation of the EBK model indicate~~s~~d the accuracy of the OC density predictions ~~in the study site.~~were ~~Results had~~ ME=~~-~~-0.27 kg/m^{3}~~-~~, and RMSE=4.21 kg/m^{3} ~~(Table 5)~~, suggesting low bias but also that the magnitude of prediction error was substantial compared to the range of the observed data (e.g., Figure 9).

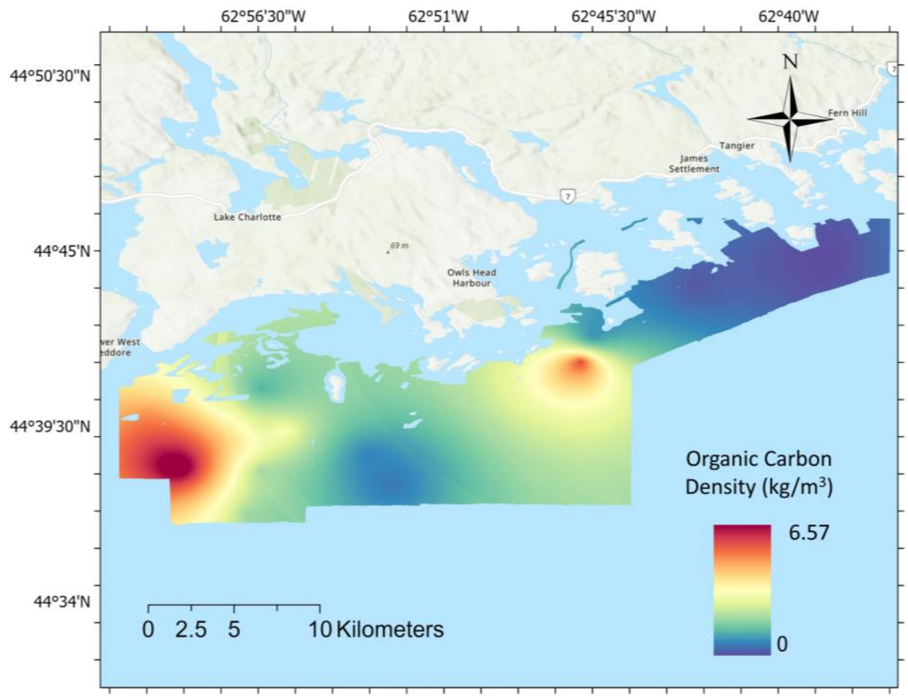

Figure 9. Spatial interpolation of OC using ~~an~~ EBK ~~method~~. ~~Low quantities of OC are represented in blue and the high quantities in red. (Basemap: Esri NASA, NGA, USGS, Province of 335 Nova Scotia Esri Canada, Esri HERE, Garmin, SafeGraph, METI/NASA, USGS, NRCan, Parks Canada).~~

The EBRK model prediction ~~demonstrates~~suggested ~~that there are~~ high ~~amounts of~~ OC density ~~found~~ in the west and south-west of the study area. ~~There is also a~~ A significant quantity of OC density was predicted ~~slightly~~ eastward near Owls Head Harbour (Figure 10). The lowest ~~amount of~~ OC density ~~is~~ was predicted at the eastern part of the study area with quantities close to zero.

Cross-~~validation~~ validation indicated ~~of the EBRK model indicated the accuracy of OC density OC (m_{OC}) predictions in the soft sediment areas. Results had~~ ME= -0.31~~0.16~~ kg/m^3 and ~~and~~ RMSE= 3.52~~7.93~~ kg/m^3, suggesting slightly higher bias than the EBK model, yet more accurate predictions ~~(Table 5)~~. ~~These results imply that the ME was close to 0 and the RMSE is small indicating a minimal biased prediction.~~

~~Table 6. Outputs from the EBRK model predicting OC density within the soft substrate. Model performance results are given by the ME= Mean error and RMSE= Root Mean Squared Error.~~

~~5. EBRK model details~~

~~No of simulation~~	~~Model selected~~	~~No of variables~~	~~ME~~	~~RMSE~~
~~100~~	~~Exponential~~	~~5~~	~~-0.31~~	~~3.52~~

~~After calculating the porosity, dry bulk density and measuring percent OC, the predicted mass of OC per unit area (m_{OC}) was determined and spatially interpolated. The spatial distribution of m_{OC} values is shown in Figure 8. The highest amount of OC concentration was found in the west of the study area along with a small patch of high concentration near Owls Head Harbour.~~

~~The EBRK model prediction demonstrates that there are high amounts of OC density found in the west and south-west of the study area. There is also a significant quantity of OC density slightly eastward near Owls Head Harbour (Figure 10). The lowest amount of OC density is the east part of the study area with quantities close to zero.~~

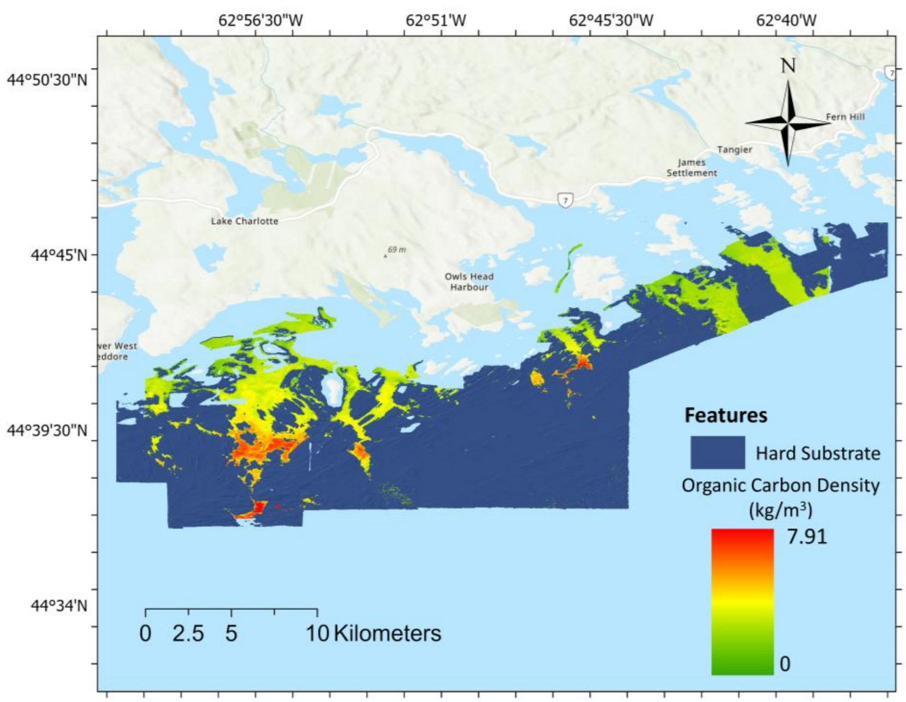

Figure 10~~8~~. Spatial interpolation of ~~organic carbon~~OC using ~~the~~ EBRK~~ method~~. ~~Low quantities of organic carbon~~OC ~~are represented by green and the high quantities by red. (Basemap: Esri NASA, NGA, USGS, Province of Nova Scotia Esri Canada, Esri HERE, Garmin, SafeGraph, METI/NASA, USGS, NRCan, Parks Canada).~~.

Table 5~~6~~. Outputs from the EBRK model predicting OC density within the soft substrate. Model performance results are given by the ME= Mean error and RMSE= Root Mean Squared Error.

No of simulation	Model selected	No of variables	ME	RMSE
100	Exponential	5	-0.31	3.52

4.5 Organic Carbon Estimates

Estimates of average OC density, OC stock per pixel and total OC stock ~~were~~ were calculated ~~from~~for all four ~~three~~ scenarios (Table 6). ~~: 1) assuming a homogeneous seafloor across the study area (i.e. lacking high-resolution~~

~~seafloor mapping data); 2) averaging OC across the soft sediment area; 3) estimating spatial heterogeneity of OC across the soft sediment area (Table 6) (supplementary material). In scenario 1, the OC samples were scaled up to the entire study area with an average estimate of 1275 Mt. In scenario 2, when using the high-resolution substrate map (assuming negligible OC in the hard substrate regions), the average m_{OC} for the study area was calculated at 259 Mt. In scenario 3, after determining the average m_{OC} found in the spatially interpolated soft sediment areas, the quantity was estimated at 203 Mt of OC (Table 6). The second two estimations assume that there is no OC within the coarse substrata and is based on the spatial extent of the soft substrate class.~~

Table 6~~6~~. Calculations used to determine the total stock of OC in the mud/sand sediment type and the total stock of OC in the entire study area.

Maps	Average density~~stock~~ of ~~organic carbon~~OC per grid cell (kg/m^3)	Average OC stock per grid cell (kg per m^2)	Total grid cells	Total stock of ~~organic carbon~~OC in study area (~~M~~t)
Scenario 1: a~~A~~ssuming homogenous seabed (entire study site)	3.62 (0.804 to 14.31)	1.45 (0.322 to 5.72)	5.58E+07	80,901 (17,949 to 319, 335)
Scenario 2: EBK m~~M~~ethod (entire study site)	2.62 (1.08 to 6.57)	1.05 (0.432 to 2.63)		58,406 (24,092 to 146,560)
Scenario 3: ~~A~~assuming heterogenous seabed (~~Soft~~ soft substrate) ~~sediments~~	3.62 (0.804 to 14.31)	1.45 (0.322 to 5.72)	1.13E+07	16,437 (3,647 to 68,882)
Scenario 4: EBRK ~~M~~method (soft substrate) ~~organic carbon~~OC ~~map~~	1.45 (0 to 7.91)	0.57 (0 to 3.16)		6,475 (0 to 35,850)

5 Discussion

Our study explores how high-resolution spatial models can improve carbon budget estimates. We have described a quantitative spatial model of hard and soft substrate ~~on~~ in a continental shelf environment and determined four~~three~~ estimates of OC stock~~total m_{OC}~~ in the surficial sediments (top 10 cm) ~~of sediments~~: scaling to the entire study area (scenario 1), interpolating OC density using an EBK model (scenario 2), scaling to only the soft substrate (scenario 3~~2~~), and ~~the~~ refining~~ed~~ m_{OC} ~~m_{OC}~~ within the soft substrate estimated from ~~the~~ an EBRK model (scenario 4~~3~~). The results demonstrate that as spatial models become more detailed, the ~~accuracy of~~ OC stock estimation increases in accuracy but decreases the overall predicted OC stock. ~~m_{OC} estimates increases, while the estimates of organic carbon~~OC ~~stock decrease substantially.~~

5.1 Evaluation of Sediment Map

The sediment map effectively classified the hard and soft substrate (kappa=0.69)~~F1=0.91~~) and significantly refined our understanding of the detailed distribution of the ~~organic carbon~~OC. Previous studies have applied similar machine learning modelling approaches with success (Stephens and Diesing ~~et al~~*et al*., 2015; Misiuk ~~et al~~*et al*., 2019; Mitchell ~~et al~~*et al*., 2019; Epstein ~~et al~~*et al*. 2023). Our results further demonstrate that this approach is suitable for mapping benthic substrates where high-resolution MBES data sets and suitable sediment ground-truthing are available. Other studies have found the highest POC concentrations are associated with gravelly mud, mud, and sandy mud ~~that the highest mass of POC was associated with gravelly mud, mud, and sandy mud areas~~ (Diesing ~~et al~~*et al*., 2017). This agrees with our linear regression ~~OLS analysis~~ that areas of increased OC have a high mud content (Figure 4). The empirical relationship observed between mud content ~~sediment grain size~~ and OC strongly suggests the importance of using substrate maps to precisely estimate the stock of OC.

5.2 Variability in Organic Carbon Stocks

Differences in estimated OC stock suggest that the substrate map was an essential component to this study. Smeaton *et al*. (2021) ~~has stated~~ note that the seafloor is commonly assumed homogenous ~~tThere is commonly an assumption~~ in benthic OC studies ~~studies that the seafloor is homogenous (Smeaton et al., 2021)~~. ~~Since s~~Shelf environments are inherently heterogeneous, and scaling up OC measurements ~~the approach applied here~~ where high-~~-~~resolution mapping data are available offers an effective way of obtaining accurate estimates of OC in ~~shelf environments~~ these areas (Snelgrove ~~et al~~*et al*., 2018). To improve estimates and better identify how the ocean carbon cycle will be altered by climate change and possibly human activities, carbon studies should embrace the full complexity of the seafloor (Snelgrove ~~et al~~*et al*., 2018; Epstein ~~et al~~*et al*., 2023). Our study ~~also~~ emphasizes the benefits of high resolution MBES data for such applications, and the need for additional coverage and collection of seafloor mapping data sets in coastal waters where coverage is currently limited (Mayer ~~et al~~*et al.*, 2018).

The difference in the total m_{OC} calculated based on the substrate map (16,437 and 6,475~~259~~ ~~M~~t of OC) versus estimates in the absence of a map (80,901 and 58,406 ~~1275 M~~t of OC) emphasizes that a spatial component to OC estimations is essential for carbon system models. This difference demonstrates the need to understand the presence of hard substrate at the seabed when calculating carbon stocks as ~~emphasized~~ suggested in recent broadscale carbon modelling studies (Epstein *et al*., 2023). Currently, global carbon models are oversimplifying carbon processes due to a ~~our~~ lack of information and data on~~understanding of~~ the complexity of the marine carbon cycle. For instance, previous studies have examined carbon quantity at the surface of the oceans by analyzing phytoplankton activity using satellite imagery, since there is an assumption that carbon at the surface of the oceans correlates with areas of high carbon storage at the seafloor (Chase ~~et al~~*et al*., 2022). This assumption ignores the complexity of carbon moving through the pelagic and benthic regions. Spatially continuous seafloor mapping data are ~~is~~ a step towards improving accuracy in our estimation, which will enhance the ongoing investigations into the marine carbon cycle.

Additionally, the resolution of the seafloor mapping data is important when modeling OC. For instance, by using a 2~~m~~-by-2 m grid resolution we can interpolate the carbon within the soft substrate using EBRK models. Through the EBRK interpolation of carbon, the carbon stock ~~total m_{OC}~~ (6,389~~203~~ Mt of OC) was less than the estimates that assume a homogenous soft substrate. The EBRK method indicates that high resolution interpolated models of OC can help to further refine standing stock estimates and provide insight into where the carbon hotspots are within the study area.

The estimates from our study were compared to the paper by Epstein et al. (2024) since they evaluated organic carbon stock in the entire Canadian continental margin, which included our study area. To compare these estimates, we clipped their OC density map to our study site and found that the mean OC density was 7.12 kg/m^3 (3.89 kg/m^3 to 11.6 kg/m^3). This mean OC density is within the range of scenarios 1, 3 (0.804 kg/m^3 to 14,31 kg/m^3), and 4 (0 kg/m^3 to 7.91 kg/m^3) presented here. To compare the total OC stock for the study region, we adjusted the depth used by Epstein et al. (2024) from 0.3 m to 0.1 m by dividing their OC stock estimates by 3. The OC stock was 161,552 t (88,183 t to 263,076 t), which is within the range of scenario 1 (17,949 t to 319, 335 t). One reason for the higher estimates in the study by Epstein et al. (2024) could be that no OC measurements within the study region were available in Epstein et al. (2024). Therefore, their model relied on OC data outside this area, which could lead to error. Furthermore, an underrepresentation of zero values in the response data could lead to an overestimation of organic carbon standing stocks in their study, as zero values are unlikely to be predicted from model outputs. The comparison between both studies highlights the importance of sediment classification maps when estimating sedimentary OC stock; knowing the extent of bedrock can reduce the overestimation of OC content substantially.

5.3 Organic Carbon Maps

When comparing the EBK and the EBRK carbon maps, there were some similarities and differences. Both maps indicate a hotspot near Owls Head Harbour and low OC density on the eastern side of the study ~~site~~area. Yet, the EBK map shows a large area of high OC density on the west side of the study area, whereas the EBRK model has a smaller area slightly east of that location. These differences between the models emphasize that the EBK model could have some inaccurate interpolation due to the limited sediment samples in the study ~~site~~area. In contrast, the EBRK model was performed in the soft substrate, where all the samples were distributed, with fewer data gaps. The EBK model indicates that without high-resolution seafloor mapping data, you can obtain a general understanding of OC hotspots. However, the EBRK model can provide a more precise understanding of the spatial variability of OC density in the study site.

Both maps suggest high OC densities associated with locations further offshore (Figures 9 & 10) and within sediments containing increased amounts of silt and sand (Figures 7 & 8). Based on previous evaluations of the study area, inshore sediment is often comprised of bedrock with patchy sand and gravel, whereas further offshore, there is thick glacial marine mud over bedrock (Fisheries and Oceans Canada, 2019). This geomorphology could be ~~why~~the cause of ~~there is~~ higher OC density further offshore. The cause of increased OC content near Owls Head Harbour remains uncertain, lacking any aquaculture or substantial runoff from nearby agriculture. However, the ESI has substantial kelp and eelgrass beds~~,~~; ~~and~~ future research may explore relationships between these environments and OC.

5.4 Limitations of the Study

The lack of dry bulk density measurements for the OC stock calculations was a major limitation of this study. The use of a dry bulk density equation derived from a previous study could introduce error into calculations based on regional geological differences. Only two seabed sediment classes were mapped here, which does not represent the actual complexity of substrate types within the ESI. Preliminary Random Forest model runs that incorporated additional sediment classes~~,~~ showed high error and poor performance, likely due to the difficulty in accurately determining sediment types from a small number of subsea video samples. We emphasize~~s~~ challenges associated with differentiating complex substrate classes that have been noted in previous similar studies (e.g., Diesing *et al.*, 2020).

We have also assumed here that there is no OC in the hard substrate. The hard substrate class included more than bedrock, with regions of mixed sediment such as gravelly mud, visible in the subsea video which could contain some OC content. Thus, improving the sediment classification map to include more complex substrates could improve the OC stock estimates further. The limited number of OC samples may have skewed the interpolation ~~of OC density~~ since the data points were not uniformly distributed within the areas of soft substrate. We therefore recommend higher sampling densities for~~,~~ future OC studies.

These limitations highlight the challenges of carbon modelling on the seafloor and the need for further research into evaluating the correct procedure for utilizing sediment classification maps when predicting OC stock. Furthermore, there is persistent uncertainty surrounding how much surface particulate OC (POC) reaches the seafloor and ~~and~~ the spatial distribution of the sinks of this material. Thus, future carbon studies should evaluate benthic-pelagic coupling and the impact it has on OC stocks.

5.5~~1~~ Future Implications of Organic Carbon M~~m~~odels

Marine spatial planners are trying to manage the seabed in a sustainable manner and high resolution regional-scale OC mapping data could be a practical option to help identify vulnerable C stores and hotspots, and to determine how these areas may be altered due to environmental change and ~~anthropocentric~~ anthropogenic activities (Hunt ~~et al~~*et al*., 2021). ~~Marine protected areas~~MPAs have been defined as regions that conserve marine resources, ecosystem services or cultural heritage (Mayr ~~et al~~*et al*., 2010). High-resolution seafloor OC models could help redefine MPAs and allow them to incorporate areas of high carbon stock~~sequestration~~. It is important to recognize sediments as long-term carbon sinks that provide climate regulation services.

It is challenging to measure how human ~~anthropocentric~~ activities like bottom trawling are impacting the seabed and how they influence OC without understanding of the natural processes of marine carbon cycling. Studies that examine OC spatially and its connections to seafloor composition are a crucial component to piecing together the natural marine carbon cycle, which can help determine if the amount of remineralization occurring from human activities will have a substantial impact on climate. Even with a relatively limited number of OC samples, this study demonstrates that high-resolution seafloor substrate maps and spatial OC models are critical to understanding the spatial heterogeneity of ~~organic carbon~~OC on the seafloor.

6 Conclusions

In this study, we generated a high-resolution sediment map that accurately captured the spatial complexity and distribution of broad sediment types in the ESI area. Through the four scenarios for estimating OC stocks, we demonstrated that seafloor sediments are a good high-resolution proxy that enable accurate estimation of OC stock in the area, and that information (or lack of information) regarding the spatial heterogeneity of the seafloor substrata substantially influences estimates of OC stock (ranging from 80,901 – 6,475 t of OC). These results emphasize that further research should explore high-resolution multibeam echosounder data in determining OC rich hotspots to improve our understanding of the role that benthic systems play as global carbon stores, and how management of these systems can contribute towards climate change management strategies and marine climate policy. ~~We have presented a method that utilizes high-resolution sedimentary maps and spatial models to quantify OC estimates. We show that examining the spatial heterogeneity of carbon content within the soft substrate can improve the estimates of organic carbon content. These results emphasize that further research should explore high-resolution multibeam echosounder data in determining OC rich hotspots to help support management measures. In this study, additional ground truthing is necessary to create more precise measurements of OC and to further evaluate which sediment type is most significant for OC storage. Despite the limited dataset, high-resolution sediment classification maps are necessary to improve our understanding of spatial patterns of OC. Additional surficial sediment OC distribution studies are necessary to improve seabed management and marine policy.~~

Data Availability

Bathymetry data was obtained from the Canadian Hydrographic Service (CHS) NONNA Portal -https://data.chs-shc.ca/login. All other data used in this study is in the supplementary material or available upon reasonable request.

Competing Interests

One of the authors is a member~~s~~ of the editorial board of *Biogeosciences*.

References

–Acharya, S. S., & Panigrahi, M. K. (2016). Evaluation of factors controlling the distribution of organic matter and phosphorus in the Eastern Arabian Shelf: A geostatistical reappraisal. Continental Shelf Research, 126, 79–88. https://doi.org/10.1016/j.csr.2016.08.001

ArcGIS Pro. (2023). *Focal Statistics (spatial analyst)*. Focal Statistics (Spatial Analyst)-ArcGIS Pro | Documentation. https://pro.arcgis.com/en/pro-app/latest/tool-reference/spatial-analyst/focal-statistics.htm

Atwood, T. B., Witt, A., Mayorga, J., Hammill, E., & Sala, E. (2020). Global Patterns in Marine Sediment Carbon Stocks. *Frontiers in Marine Science*, *7*, 165. https://doi.org/10.3389/fmars.2020.00165

Berner, R.A. (2003) 'The long-term carbon cycle, fossil fuels and atmospheric composition', Nature, 426, pp. 323–326. Available at: https://doi.org/https://doi.org/10.1038/nature02131.Bianchi, T.S., Aller, R.C., Atwood, T.B., Brown, C.J., Buatois, L.A., Levin, L.A., Levinton, J.S., Middelburg, J.J., Morrison, E.S., Regnier, P., Shields, M.R., Snelgrove, P.V., Sotka, E.E., & Stanley, R.R. (2021). What global biogeochemical consequences will marine animal–sediment interactions have during climate change? Elementa: Science of the *Anthropocene* 9: 1. doi.10.1525/elementa.2020.00180

Bianchi, T. S., Brown, C. J., Snelgrove, P. V. R., Stanley, R. R. E., Cote, D., & Morris, C. (2023). Benthic Invertebrates on the Move: A Tale of Ocean Warming and Sediment Carbon Storage. *Limnology and Oceanography Bulletin*, *32*(1), 1–5. https://doi.org/10.1002/lob.10544

Bondt, G. (2019). Final Field report for the Eastern Shore Islands. CHSDIR Project Number: 2901633 1001-07-F01_2901633_2602567_EasternShore_FFR%20(1).pdf

Bondt, G. (2020). Final Field report for the Eastern Shore Islands. CHSDIR Project Number: 9000294 9000713_1001-07-F01_9000294_EasternShore_2020_Field%20Report%20(1).pdf

Boumpoulis, V., Michalopoulou, M. & Depountis, N. (2023). Comparison between different spatial interpolation methods for the development of sediment distribution maps in coastal areas. *Earth Sci Inform* **16**, 2069–2087. https://doi.org/10.1007/s12145-023-01017-4

Brown, C. J., Smith, S. J., Lawton, P., & Anderson, J. T. (2011). Benthic habitat mapping: A review of progress towards improved understanding of the spatial ecology of the seafloor using acoustic techniques. *Estuarine, Coastal and Shelf Science*, *92*(3), 502–520. https://doi.org/10.1016/j.ecss.2011.02.007

Brown, D. R., Conrad, S., Akkerman, K., Fairfax, S., Fredericks, J., Hanrio, E., Sanders, L. M., Scott, E., Skillington, A., Tucker, J., Van Santen, M. L., & Sanders, C. J. (2016). Seagrass, mangrove and saltmarsh sedimentary carbon stocks in an urban estuary; Coffs Harbour, Australia. *Regional Studies in Marine Science*, *8*, 1–6. https://doi.org/10.1016/j.rsma.2016.08.005

Buhl-Mortensen, P., Lecours, V., & Brown, C. J. (2021). Editorial: Seafloor Mapping of the Atlantic Ocean. *Frontiers in Marine Science*, *8*, 721602. https://doi.org/10.3389/fmars.2021.721602

Burdige, D. J. (2007). Preservation of Organic Matter in Marine Sediments: Controls, Mechanisms, and an Imbalance in Sediment Organic Carbon Budgets? *Chemical Reviews*, *107*(2), 467–485. https://doi.org/10.1021/cr050347qChase, A. P., Boss, E. S., Haëntjens, N., Culhane, E., Roesler, C., & Karp-Boss, L. (2022). Plankton

Imagery Data Inform Satellite-Based Estimates of Diatom Carbon. *Geophysical Research Letters*, *49*(13). https://doi.org/10.1029/2022GL098076

Collier, J. S., and Brown, C. J. (2005). Correlation of sidescan backscatter with grain size distribution of surficial seabed sediments. *Mar. Geol.* 214, 431–449. doi: 10.1016/j.margeo.2004.11.011

Dahl, M, Deyanova, D, Gütschow, S, Asplund, ME, Lyimo, LD, et al. (2016) Sediment Properties as Important Predictors of Carbon Storage in Zostera marina Meadows: A Comparison of Four European Areas. PLOS ONE 11(12): e0167493. https://doi.org/10.1371/journal.pone.0167493

Diesing, M., Kröger, S., Parker, R., Jenkins, C., Mason, C., & Weston, K. (2017). Predicting the standing stock of organic carbon in surface sediments of the North–West European continental shelf. *Biogeochemistry*, *135*(1–2), 183–200. https://doi.org/10.1007/s10533-017-0310-4

Diesing, M., Mitchell, P.J., O'Keeffe, E., Gavazzi, G.O.A.M., Bas, T.L. (2020). Limitations of Predicting Substrate Classes on a Sedimentary Complex but Morphologically Simple Seabed. *Remote Sensing* 12, 3398. https://doi.org/10.3390/rs12203398

Diesing, M., Thorsnes, T., and Bjarnadóttir, L. R. (2021). Organic carbon densities and accumulation rates in surface sediments of the North Sea and Skagerrak, Biogeosciences, 18, 2139–2160, https://doi.org/10.5194/bg-18-2139-2021, 2021.

Epstein, G., Middelburg, J. J., Hawkins, J. P., Norris, C. R., & Roberts, C. M. (2022). The impact of mobile demersal fishing on carbon storage in seabed sediments. *Global Change Biology*, *28*(9), 2875–2894. https://doi.org/10.1111/gcb.16105Epstein, G., Fuller, S. D., Hingmire, D., Myers, P. G., Peña, A., Pennelly, C., and Baum, J. K. (2024). Predictive mapping of organic carbon stocks in surficial sediments of the Canadian continental margin, Earth Syst. Sci. Data, 16, 2165–2195, https://doi.org/10.5194/essd-16-2165-2024.Feng, T., Stanley, R. R. E., Wu, Y., Kenchington, E., Xu, J., & Horne, E. (2022). A High-Resolution 3-D Circulation Model in a Complex Archipelago on the Coastal Scotian Shelf. Journal of Geophysical Research. Oceans, 127(3). https://doi.org/10.1029/2021JC017791

Fennel, K., Alin, S., Barbero, L., Evans, W., Bourgeois, T., Cooley, S., Dunne, J., Feely, R. A., Hernandez-Ayon, J. M., Hu, X., Lohrenz, S., Muller-Karger, F., Najjar, R., Robbins, L., Shadwick, E., Siedlecki, S., Steiner, N., Sutton, A., Turk, D., … Wang, Z. A. (2019). Carbon cycling in the North American coastal ocean: A synthesis. *Biogeosciences*, *16*(6), 1281–1304. https://doi.org/10.5194/bg-16-1281-2019

Fisheries and Oceans Canada (2019). Biophysical and Ecological Overview of the Eastern Shore Islands Area of Interest (AOI). DFO Can. Sci. Advis. Sec. Sci. Advis. Rep. 2019/016.

Giustini, F., Ciotoli, G., Rinaldini, A., Ruggiero, L., & Voltaggio, M. (2019). Mapping the geogenic radon potential and radon risk by using Empirical Bayesian Kriging regression: A case study from a volcanic area of central Italy. The Science of the Total Environment, 661, 449–464. https://doi.org/10.1016/j.scitotenv.2019.01.146

Goff, J. A., Olson, H. C., and Duncan, C. S. (2000). Correlation of side-scan backscatter intensity with grain-size distribution of shelf sediments, New Jersey margin. *Geo Mar. Lett.* 20, 43–49. doi: 10.1007/s003670000032

Haar, C.D., Misiuk, B., Gazzola, V., Wells, M., Brown, CJ. (2023). Harmonizing multi-source backscatter data to generate regional seabed maps: Bay of Fundy, Canada. Journal of Maps. 19 (1) doi.10.1080/17445647.2023.222362

Hedges, J. I., & Keil, R. G. (1995). Sedimentary organic matter preservation: An assessment and speculative synthesis. *Marine Chemistry*.

Hilborn, R., Amoroso, R., Collie, J., Hiddink, J. G., Kaiser, M. J., Mazor, T., McConnaughey, R. A., Parma, A. M., Pitcher, C. R., Sciberras, M., & Suuronen, P. (2023). Evaluating the sustainability and environmental impacts of trawling compared to other food production systems. *ICES Journal of Marine Science*, fsad115. https://doi.org/10.1093/icesjms/fsad115

Hilmi, N., Chami, R., Sutherland, M. D., Hall-Spencer, J. M., Lebleu, L., Benitez, M. B., & Levin, L. A. (2021). The Role of Blue Carbon in Climate Change Mitigation and Carbon Stock Conservation. *Frontiers in Climate*, *3*, 710546. https://doi.org/10.3389/fclim.2021.710546

Howard, J., Sutton-Grier, A. E., Smart, L. S., Lopes, C. C., Hamilton, J., Kleypas, J., Simpson, S., McGowan, J., Pessarrodona, A., Alleway, H. K., and Landis, E. (2023). Blue Carbon pathways for climate mitigation: Known, emerging and unlikely, Mar Policy, 156, 105788, https://doi.org/https://doi.org/10.1016/j.marpol.2023.105788, 2023.

Huang, Z., Nichol, S. L., Siwabessy, J. P., Daniell, J., & Brooke, B. P. (2012). Predictive modelling of seabed sediment parameters using multibeam acoustic data: a case study on the Carnarvon Shelf, Western Australia. *International Journal of Geographical Information Science*, *26*(2), 283-307.

Hunt, C. A., Demšar, U., Marchant, B., Dove, D., & Austin, W. E. N. (2021). Sounding Out the Carbon: The Potential of Acoustic Backscatter Data to Yield Improved Spatial Predictions of Organic Carbon in Marine Sediments. *Frontiers in Marine Science*, *8*, 756400. https://doi.org/10.3389/fmars.2021.756400

Hunt, C., Demšar, U., Dove, D., Smeaton, C., Cooper, R., & Austin, W. E. N. (2020). Quantifying Marine Sedimentary Carbon: A New Spatial Analysis Approach Using Seafloor Acoustics, Imagery, and Ground-Truthing Data in Scotland. *Frontiers in Marine Science*, *7*, 588. https://doi.org/10.3389/fmars.2020.00588

IPCC. (2019). Annex I: Glossary [Weyer, N.M. (ed.)]. In: IPCC Special Report on the Ocean and Cryosphere in a Changing Climate [H.-O. Pörtner, D.C. Roberts, V. Masson-Delmotte, P. Zhai, M. Tignor, E. Poloczanska, K. Mintenbeck, A. Alegría, M. Nicolai, A. Okem, J. Petzold, B. Rama, N.M. Weyer (eds.)]. Cambridge University Press, Cambridge, UK and New York, NY, USA, pp. 677–702. https://doi.org/10.1017/9781009157964.010.

Jenkins C (2005) Summary of the on-CALCULATION methods used in dbSEABED. http://pubs.usgs.gov/ds/2006/146/ docs/onCALCULATION.pdf. Accessed 27 July 2023

Krause,J.R., Hinojosa-Corona, A., Gray, A.B., Herguera,J.C., McDonnell, J., Schaefer, M.V., Ying,S.C., Watson, E.B. (2022). Beyond habitat boundaries: Organic matter cycling requires a system-wide approach for accurate blue carbon accounting. *Limnology and Oceanography*. 9999: 1-13. doi: 10.1002/lno.12071

King, E. L. (2018). *Surficial geology and features of the inner shelf of eastern shore, offshore Nova Scotia* (8375; p. 8375). https://doi.org/10.4095/308454

Krivoruchko K, Gribov A. (2019). Evaluation of empirical Bayesian kriging. Spat Stat 32:. https://doi.org/10.1016/j.spasta.2019.100368

Legge, O., Johnson, M., Hicks, N., Jickells, T., Diesing, M., Aldridge, J., Andrews, J., Artioli, Y., Bakker, D. C. E., Burrows, M. T., Carr, N., Cripps, G., Felgate, S. L., Fernand, L., Greenwood, N., Hartman, S., Kröger, S., Lessin, G., Mahaffey, C., … Williamson, P. (2020). Carbon on the Northwest European Shelf: Contemporary Budget and Future Influences. *Frontiers in Marine Science*, *7*, 143. https://doi.org/10.3389/fmars.2020.00143

Liaw, A., Wiener, M.. (2002). Classification and regression by randomForest. R news 2, 18–22.

Lovelock, C. E. and Duarte, C. M. (2019). Dimensions of Blue Carbon and emerging perspectives, Biol Lett, 15, 20180781, https://doi.org/10.1098/rsbl.2018.0781, 2019.

Lucieer, V., Hill, N. A., Barrett, N. S., & Nichol, S. (2013). Do marine substrates 'look'and 'sound'the same? Supervised classification of multibeam acoustic data using autonomous underwater vehicle images. *Estuarine, Coastal and Shelf Science*, *117*, 94-106.

Mallik, S., Bhowmik, T., Mishra, U., & Paul, N. (2022). Mapping and prediction of soil organic carbon by an advanced geostatistical technique using remote sensing and terrain data. Geocarto International, 37(8), 2198–2214. https://doi.org/10.1080/10106049.2020.1815864

Mason C. (2011). NMBAQC's Best Practice Guidance. Particle Size Analysis (PSA) for Supporting Biological Analysis. National Marine Biological AQC Coordinating Committee.

Mayer, L., Jakobsson, M., Allen, G., Dorschel, B., Falconer, R., Ferrini, V., Lamarche, G., Snaith, H., Weatherall, P. (2018). The Nippon Foundation—GEBCO Seabed 2030 Project: The Quest to See the World's Oceans Completely Mapped by 2030. Geosciences. 8(2):63. doi:10.3390/geosciences8020063.

Mayr, F. B., Upton, H. F. (Harold F., Buck, E. H., Upton, H. F. (Harold F., & Vann, A. (2010). Marine protected areas. Nova Science Publishers.

McHugh ML. Interrater reliability: the kappa statistic. Biochem Med (Zagreb). 2012;22(3):276-82. PMID: 23092060; PMCID: PMC3900052.

McLeod, E. *et al*. (2011) 'A blueprint for Blue Carbon: Toward an improved understanding of the role of vegetated coastal habitats in sequestering CO2', rontiers in Ecology and the Environment, 9(10), pp. 552–560. Available at: https://doi.org/10.1890/110004.

Middelburg, JJ. (2018). Reviews and syntheses: To the bottom of carbon processing at the seafloor. Biogeosciences 15: 413–427. DOI: http://dx.doi.org/10.5194/bg-15-413-2018.

Misiuk, B, Brown, C.J. (2023). Benthic habitat mapping: A review of three decades of mapping biological patterns on the seafloor. Estuarine Coastal and Shelf Science. In Press

Misiuk, B., Brown, C.J., Robert, K., Lacharite, M. (2020). Harmonizing multi-source sonar backscatter datasets for seabed mapping using bulk shift approaches. Remote Sensing. 12(4): 601. https://doi.org/10.3390/rs12040601

Misiuk, B., Diesing, M., Aitken, A., Brown, C. J., Edinger, E. N., & Bell, T. (2019). A spatially explicit comparison of quantitative and categorical modelling approaches for mapping seabed sediments using random forest. Geosciences (Basel), 9(6), 254–. https://doi.org/10.3390/geosciences9060254

Misiuk, B., Lacharité, M., Brown, C.J. (2021). Assessing the use of harmonized multisource backscatter data for thematic benthic habitat mapping. Science of Remote Sensing. 3. doi.10.1016/j.srs.2021.1000

Mitchell, P. J., Aldridge, J., & Diesing, M. (2019). Legacy data: How decades of seabed sampling can produce robust predictions and versatile products. Geosciences (Basel), 9(4), 182–. https://doi.org/10.3390/geosciences9040182

Mollenhauer G, Schneider RR, Jennerjahn T *et al* (2004). Organic carbon accumulation in the South Atlantic Ocean: its modern, mid-Holocene and last glacial distribution. Glob Planet C

Najjar, R. G., Herrmann, M., Alexander, R., Boyer, E. W., Burdige, D. J., Butman, D., Cai, W. -J., Canuel, E. A., Chen, R. F., Friedrichs, M. A. M., Feagin, R. A., Griffith, P. C., Hinson, A. L., Holmquist, J. R., Hu, X., Kemp, W. M., Kroeger, K. D., Mannino, A., McCallister, S. L., … Zimmerman, R. C. (2018). Carbon Budget of Tidal Wetlands, Estuaries, and Shelf Waters of Eastern North America. *Global Biogeochemical Cycles*, *32*(3), 389–416. https://doi.org/10.1002/2017GB005790

Oceans North. (2024). Mapping Carbon in Canada's Seafloor. https://www.oceansnorth.org/wp-content/uploads/2024/05/Seabed-Mapping-Policy-Brief-May2024_final2.pdf

Pellicone G, Caloiero T, Modica G, Guagliardi I. (2018). Application of several spatial interpolation techniques to monthly rainfall data in the Calabria region (southern Italy). Int J Climatol 38:3651–3666. https://doi.org/10.1002/joc.5525

Sala, E., Mayorga, J., Bradley, D., Cabral, R. B., Atwood, T. B., Auber, A., Cheung, W., Costello, C., Ferretti, F., Friedlander, A. M., Gaines, S. D., Garilao, C., Goodell, W., Halpern, B. S., Hinson, A., Kaschner, K., Kesner-Reyes, K., Leprieur, F., McGowan, J., … Lubchenco, J. (2021). Protecting the global ocean for biodiversity, food and climate. *Nature*, *592*(7854), 397–402. https://doi.org/10.1038/s41586-021-03371-z

Serrano, O., Lavery, P. S., Duarte, C. M., Kendrick, G. A., Calafat, A., York, P. H., Steven, A., and Macreadie, P. I. (2016). Can mud (silt and clay) concentration be used to predict soil organic carbon content within seagrass ecosystems?, Biogeosciences, 13, 4915–4926, https://doi.org/10.5194/bg-13-4915-2016, 2016.

smeaton, D. G., & Snellen, M. (2009). A Bayesian approach to seafloor classification using multi-beam echo-sounder backscatter data. *Applied Acoustics*, *70*(10), 1258-1268.

Smeaton, C., & Austin, W. E. N. (2019). Where's the Carbon: Exploring the Spatial Heterogeneity of Sedimentary Carbon in Mid-Latitude Fjords. *Frontiers in Earth Science*, *7*, 269. https://doi.org/10.3389/feart.2019.00269

Smeaton, C., Yang, H., & Austin, W. E. N. (2021). Carbon burial in the mid-latitude fjords of Scotland. *Marine Geology*, *441*, 106618. https://doi.org/10.1016/j.margeo.2021.106618

Snelgrove, P. V. R., Soetaert, K., Solan, M., Thrush, S., Wei, C.-L., Danovaro, R., Fulweiler, R. W., Kitazato, H., Ingole, B., Norkko, A., Parkes, R. J., & Volkenborn, N. (2018). Global Carbon Cycling on a Heterogeneous Seafloor. *Trends in Ecology & Evolution*, *33*(2), 96–105. https://doi.org/10.1016/j.tree.2017.11.004

Sokal RR, Rohlf FJ. (1981). Biometry. San Francisco, USA

Stephens, D., & Diesing, M. (2014). A comparison of supervised classification methods for the prediction of substrate type using multibeam acoustic and legacy grain-size data. *PloS one*, *9*(4), e93950.

Stephens, D., & Diesing, M. (2015). Towards quantitative spatial models of seabed sediment composition. PloS One, 10(11), e0142502–e0142502. https://doi.org/10.1371/journal.pone.0142502

Sutherland, T. F., Galloway, J., Loschiavo, R., Levings, C. D., and Hare, R. (2007). Calibration techniques and sampling resolution requirements for groundtruthing multibeam acoustic backscatter (EM3000) and QTC VIEW™ classification technology. *Estuar. Coast. Shelf Sci.* 75, 447–458. doi: 10.1016/j.ecss.2007.05.045

Vandermeulen, H. (2018). *A Drop Camera Survey of the Eastern Shore Archipelago, Nova Scotia*. Canadian Technical Report of Fisheries and Aquatic Sciences 3258. https://publications.gc.ca/collections/collection_2018/mpo-dfo/Fs97-6-3258-eng.pdf

Verardo, D. J., Froelich, P. N., & McIntyre, A. (1990). Determination of organic carbon and nitrogen in marine sediments using the Carlo Erba NA-1500 analyzer. *Deep Sea Research Part A. Oceanographic Research Papers*, *37*(1), 157–165. https://doi.org/10.1016/01980149(90)90034-S